Dispersion and 3-Picoline Ammoxidation Investigation of V₂O₅/α-Al₂O₃ Catalysts†

Benjaram Narasimha Reddy, Benjaram Mahipal Reddy and Machiraju Subrahmanyam
Catalysis Section, Indian Institute of Chemical Technology, Hyderabad 500 007, India

The effect of changing the precursor on the dispersion and 3-picoline ammoxidation activity of various α-Al₂O₃ supported V₂O₅ catalysts has been investigated by the techniques of X-ray fluorescence, AES, SEM, EPR, XRD, oxygen chemisorption at 195 K and ammonia chemisorption at 423 K. The nature of the precursor plays an important role in obtaining a highly selective catalyst for 3-picoline ammoxidation to nicotinonitrile. Using maximum oxygen uptake at 195 K and also surface-specific AES and SEM vanadium(III) acetyl-acetonate derived catalysts were found to give a highly dispersed and highly selective catalyst series for nicotinonitrile production in the title reaction. From AES study the oxygen peak intensity, which also reflects the extent of oxidation of the surface, was found to decrease in the order vanadium(III) acetylacetonate > vanadyl oxalate > ammonia meta-vanadate. The same trend was also observed in their catalytic activity in 3-picoline ammoxidation. The acidity of various catalysts, measured by ammonia uptake, correlated with their selectivity to pyridine.

The present performance of any heterogeneous catalyst is partly judged by means of its past history,[1] particularly by the method of preparation adopted for its final form of use. One of the important variables during the preparation of any supported metal oxide catalyst is the nature of the oxide component precursor.[2–7] Supported vanadia-based oxides have been recognised as selective oxidation and ammoxidation catalysts for various aliphatic, aromatic and heterocyclic hydrocarbons and are receiving more and more attention regarding their nature and dispersion of active phases on different supports.[8–11] The most efficient utilization of supported vanadia catalysts depends on the dispersion of the active phase on the surface of the support material. The actual state and dispersion of the vanadium active component on the surface of a support depends mainly on the method of preparation, nature of precursors, amount of active component and the type of support material. The extent of interaction of various vanadium precursors and the resulting dispersion and nature of vanadia phase on low-surface-area supports, e.g. α-Al₂O₃, has not been demonstrated although such studies have been reported with other supports of variable surface areas.[12–28]

In an earlier communication[29] we have shown, with the help of oxygen chemisorption measurements, that the vanadium(III) acetylacetonate was an important precursor for obtaining highly dispersed V oxide catalysts on an α-Al₂O₃ support for ammoxidation of 3-picoline. In this study we substantiate the earlier observation with more features shown by AES, SEM, EPR, XRD and ammonia chemisorption in addition to oxygen-uptake measurements. The study has been directed towards the nature, dispersion and morphologies of various V oxide catalysts obtained via three different precursors on the α-Al₂O₃ support. Conclusions are drawn from the features shown by these techniques giving particular attention to explanations of the disparities in activities and selectivities of these various catalysts in 3-picoline ammoxidation reaction.

Experimental

Catalyst Preparation

The α-Al₂O₃ support was obtained by heating γ-Al₂O₃ (Harshaw Al III-61E, S.A. 204 m² g⁻¹) at 1373 K for 12 h. The corundum phase was confirmed by X-ray diffraction analysis and gave an N₂ B.E.T. surface area of 5.1 m² g⁻¹. A standard BSS 18–25 mesh fraction of this phase was taken for impregnating the vanadium precursors. A series of α-Al₂O₃-supported vanadium catalysts with V loadings ranging from 0.5 to 6.5 wt.% were prepared by the standard wet impregnation technique with stoichiometric aqueous solutions of ammonium metavanadate (AMV), vanadyl oxalate (VOX, obtained by reducing AMV aqueous solution with oxalic acid until it gave a blue medium) and non-aqueous vanadium(III) acetylacetonate (VAA). The impregnated samples were oven-dried at 393 K for 12 h and calcined at 773 K for 6 h in a dry air atmosphere. The vanadium content was determined by X-ray fluorescence and is expressed in the text as V₂O₅ wt.% on the support. The colour, composition and B.E.T. surface area of all the catalysts are given in Table 1.

X-Ray Fluorescence

Measurements were made on a Philips PW 1400 microprocessor controlled, sequential X-ray fluorescence spectrometer with 100 kVA X-ray generator. For the analysis of vanadium content, sample pellets were prepared by pressing the catalyst powder with a backing of boric acid in collapsible aluminium cups at 20 tonnes of pressure to give pellets of 40 mm diameter. A flow detector was used to count the X-ray photons. A Philips PW 951 on-line dedicated computer was used for the regression analysis, to prepare calibration curves of intensity vs. vanadium content of various catalyst samples. The vanadium content thus obtained was converted into V₂O₅ loading (wt.%) on the support as given in Table 1.

Auger Electron Spectroscopy

The Auger spectra were obtained by a single-pass cylindrical mirror analyser (CMA) equipped with a coaxial electron gun (Physical Electronics, 545 C). The excitation was carried with a 10 kV beam under UHV (10⁻¹⁰ Torr)† conditions and the analysed kinetic energy of ejected Auger electrons ranged from 0 to 2000 eV.

Scanning Electron Microscopy

SEM investigations of catalysts were performed with a Hitachi Model SF-20 scanning electron microscope at an applied voltage of 20 kV.

---

† 1 Torr ≈ 133.3 Pa.

Table 1   Characteristics of the three series of catalysts

| | unreduced catalyst | | | reduced catalyst | |
colour	V_2O_5 /wt.%[a]	B.E.T. surface area /$m^2 g^{-1}$		B.E.T. surface area /$m^2 g^{-1}$	active-site density[b] /nm^{-2}
			AMV series		
light orange	2.22	5.4		4.5	2.19
orange	4.14	5.9		5.0	2.21
orange	6.10	6.4		5.6	2.24
orange	7.98	6.0		5.9	2.30
orange	9.57	7.2		4.7	3.10
			VOX series		
light orange	2.23	5.2		4.6	2.85
orange	4.73	5.6		4.8	3.13
orange	6.85	6.2		5.1	3.30
orange	9.46	6.5		5.6	3.46
orange	11.14	7.8		5.7	3.50
			VAA series		
grey-green	0.98	5.2		4.5	3.82
light green	2.21	5.8		4.6	3.95
light green	3.27	6.3		4.8	4.10
light green	4.03	6.8		4.7	4.45
dark green	5.01	7.7		4.9	4.52

[a] The balance was α-Al_2O_3. [b] This is equal to the number of oxygen atoms chemisorbed per unit area of the reduced catalyst.

EPR

A Bruker ER 200D-SRC X-band spectrometer was used for EPR studies of the catalysts in their same mesh fraction as used for activity measurements. The spectra were recorded at room temperature in 3 mm i.d. impurity-free quartz tubes.

X-Ray Diffraction

X-Ray diffraction analyses were made on a Philips PW 1051 X-ray diffractometer with nickel-filtered Cu-Kα radiation ($\lambda = 1.54187$ Å).

Oxygen Chemisorption

Measurements were carried volumetrically in an all-glass high-vacuum (1×10^{-6} Torr) adsorption unit with the option of *in situ* reduction with hydrogen.[30] After the chemisorption experiment the B.E.T. surface area of the catalyst was determined by N_2 adsorption at 77 K by taking 0.162 nm^2 as the cross-section of N_2 molecule. The B.E.T. surface areas of the reduced and unreduced catalysts are given in Table 1.

Ammonia Chemisorption Measurements

Ammonia chemisorption was carried out volumetrically in the same apparatus as used for oxygen chemisorption. In a typical experiment *ca.* 0.5 g of catalyst sample was degassed at 673 K (1.0×10^{-6} Torr) for 2 h. The sample temperature was then brought down to 423 K under vacuum. Ammonia gas from a storage bulb was allowed to contact the sample for 30 min. The exact equilibrium pressure and volume of this dose was noted. Several such doses have been introduced into the catalyst chamber to generate the first isotherm representing the chemisorbed and physisorbed ammonia. After this the sample was evacuated to a pressure of 1.0×10^{-6} Torr for *ca.* 3–4 h to remove completely the physically adsorbed ammonia. The second isotherm, representing only physisorbed gas, was generated immediately, in the same way as
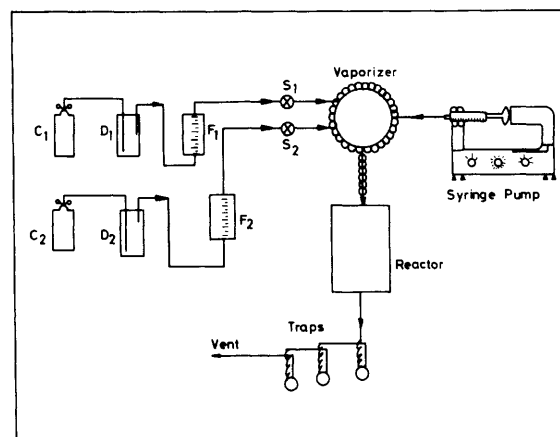

Fig. 1 Schematic diagram of the dynamic flow reactor used for the ammoxidation of 3-picoline. C_1 and C_2 are air and ammonia cylinders, respectively. D_1 and D_2 are driers. S_1 and S_2, F_1 and F_2 are stopcocks and flow metres, respectively

the first isotherm, and fell below the first under identical pressure ranges. The difference between these two isotherms was taken as a measure of volume of chemisorbed ammonia.

Catalytic Activity Measurements

The vapour-phase ammoxidation of 3-picoline was conducted in a fixed-bed vertical flow micro-reactor at atmospheric pressure at a temperature of 648 K. *Ca.* 1 g (average particle size 0.71 mm) of the fresh catalyst was packed every time between layers of quartz wool in a glass reactor (12 mm i.d.) filled with glass chips. 3-Picoline was fed through a calibrated syringe pump into a vaporizer where it was allowed to mix continuously with air and ammonia before entering the pre-heating zone of the reactor. The reactor set-up is shown schematically in Fig. 1. The molar ratio of the feed maintained was 3-picoline: NH_3: air = 1:2:20 and fed at a total rate of 100–150 mmol h^{-1}. The liquid products collected through spiral condensers in ice-cooled freezing traps were analysed by the FID of a gas chromatograph with a 30% SE-30 on A. W. Chromosorb W column kept at 413 K. The various products observed were mainly nicotinonitrile and pyridine with some traces of carbon oxides. Under steady-state conditions and in the absence of any diffusional effects, the rate of 3-picoline ammoxidation was measured using the expression $x = r(W/F)$, where r is the rate in mmol h^{-1} g^{-1} catalyst, x is the fraction of 3-picoline converted, W is the weight of catalyst in g and F is the total flow rate of all the reactants in mmol h^{-1}. The rates obtained, with conversions of 15–20%, were extrapolated to zero time so as to represent the initial state of the catalysts. The selectivity of the catalysts is expressed in terms of the fraction of 3-picoline converted to either nicotinonitrile or pyridine per hour per gram of catalyst.

Results and Discussion

AES Studies

In the present investigation the supported vanadia catalysts were used without any modification for recording AES spectra. Representative spectra of main Auger electron transitions of vanadium and oxygen of the three catalysts derived from the three different precursors are shown in Fig. 2. Similar spectra were also observed with varying intensities for all the other individual catalyst samples. A good account of work can be found in literature on the application of AES technique to the study of vanadia catalysts especially vanadia
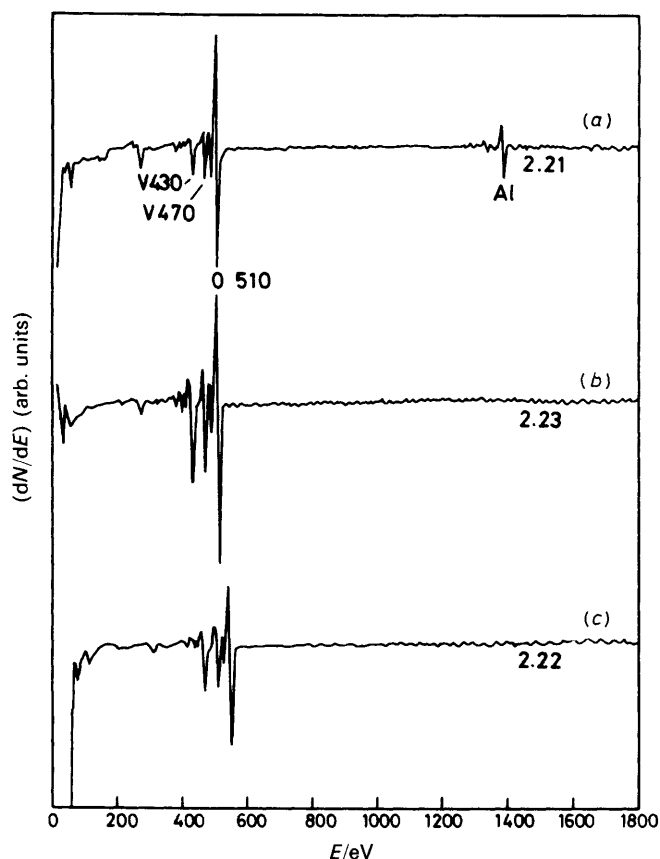
Fig. 2 Representative AES spectra of the three catalysts derived from the three different precursors: (a) VAA derived; (b) VOX derived; (c) AMV derived

Fig. 3 AES O:V ratio as a function of V_2O_5 wt.% on the support: ●, VAA series; ▼, VOX series; ○, AMV series

films[31-33] and bulk vanadium oxide.[34] In a simple interpretation, the AES studies can give some meaningful information about the dispersion of vanadia phase on the support.[35] Based on the relative intensities,[36] it appears from Fig. 2 that the extent of surface oxidation is more in the VAA-derived sample than in the other two series of samples. This is possible only when the surface dispersion of vanadia is maximum on the support. The vanadia loading (wt.%) on the support of each sample is given just below the respective spectral lines at the right end. The presence of a small Al peak at ca. 1400 eV for the VAA-derived sample results from a marginal decrease in vanadia content of this sample compared with the other two samples. In a semi-quantitative approach the O : V peak-to-peak ratios obtained from the AES spectra are plotted in Fig. 3 as a function of vanadia loading (sensitivity factor for vanadium was obtained from a standard Auger spectrum published by Palmberg et al.[37] assuming the sensitivity of oxygen to be unity). It is interesting to note that the intensity ratios calculated are distinctly different for the three series of catalysts. Fig. 3 shows that the three series of catalysts show three different lines with the experimentally determined O : V ratio decreasing with V_2O_5 loading, but tending to level off at higher concentration. The O : V ratio of the supported V-oxide shows a parabolic decrease with V_2O_5 content which can be attributed to the formation of a highly dispersed vanadia monolayer due to carrier–catalyst interaction in the lower loading region and the formation of bulky crystallites of V_2O_5 at higher loadings.[29] The surface enrichment with vanadium of high dispersion is more pronounced in the case of VAA complex derived V_2O_5/α-Al_2O_3 catalysts. These trends of dispersion were also reflected in their oxygen uptake capacities on pre-reduced surfaces and catalytic activities in 3-picoline ammoxidation reaction as discussed later.
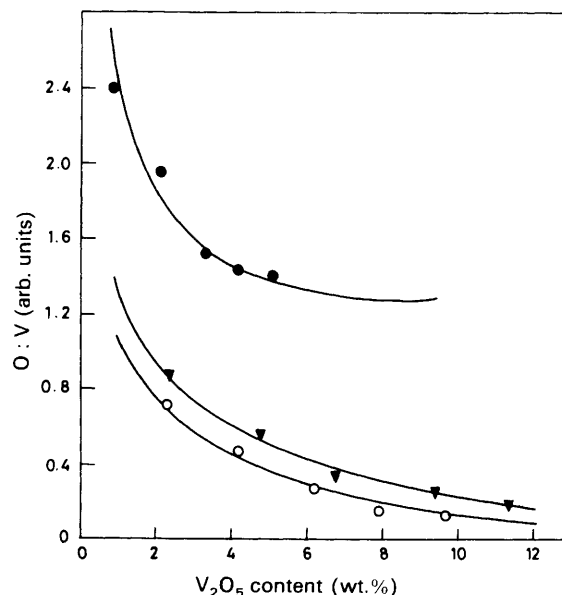
SEM and XRD Studies

All the samples were examined in a scanning electron microscope to obtain information about the surface dispersion of vanadia of various catalysts. Representative electron micrographs of the three catalysts of different origin along with pure α-Al_2O_3 are shown in Fig. 4. The electron micrograph of pure α-Al_2O_3 [Fig. 4(d)] shows that its structure closely resembles that of VAA-derived catalysts. This observation indicates that in the VAA-derived catalyst sample the vanadia phase is in a more highly dispersed state than the other two sources of catalysts. The other two catalysts show small aggregates of microcrystals[38] covering the surface of support less uniformly.

The VAA-derived series of catalysts showed characteristic XRD patterns of V_2O_5 above ca. 4.03 wt.% vanadia loadings only. However, the other two series of catalysts showed characteristic V_2O_5 XRD peaks below this loading, confirming the microcrystalites detected by SEM. The absence of characteristic V_2O_5 XRD peaks at lower loadings in the case of VAA-derived samples may be due to either high dispersion of the V oxide phase on the support surface or the crystallites formed being smaller than 4 nm, i.e. beyond the detection limit of XRD technique. The SEM results support the former possibility.

EPR Studies

The EPR signals from the paramagnetic species of V_2O_5/α-Al_2O_3 catalysts obtained at room temperature implied a very strong tetragonal–trigonal distortion of the octahedral–tetrahedral crystal field. Typical EPR spectra at low vanadia loadings of the catalysts (Fig. 5) derived from the three vanadium precursors (the wt.% loadings of V_2O_5 are shown just below the respective spectral lines on the right-hand side) show a difference for VAA- and VOX-derived samples in terms of the presence of an additional broad signal superimposed on the well resolved features of the AMV-derived sample. The spectra obtained for low vanadia contents of both AMV- and VOX-derived catalysts gradually merged to give a broad asymmetric signal with g values approaching 1.978 towards higher loadings. The VAA series of samples retained the broad resonance shoulder even at high loadings, indicating that the dispersion of vanadia phase
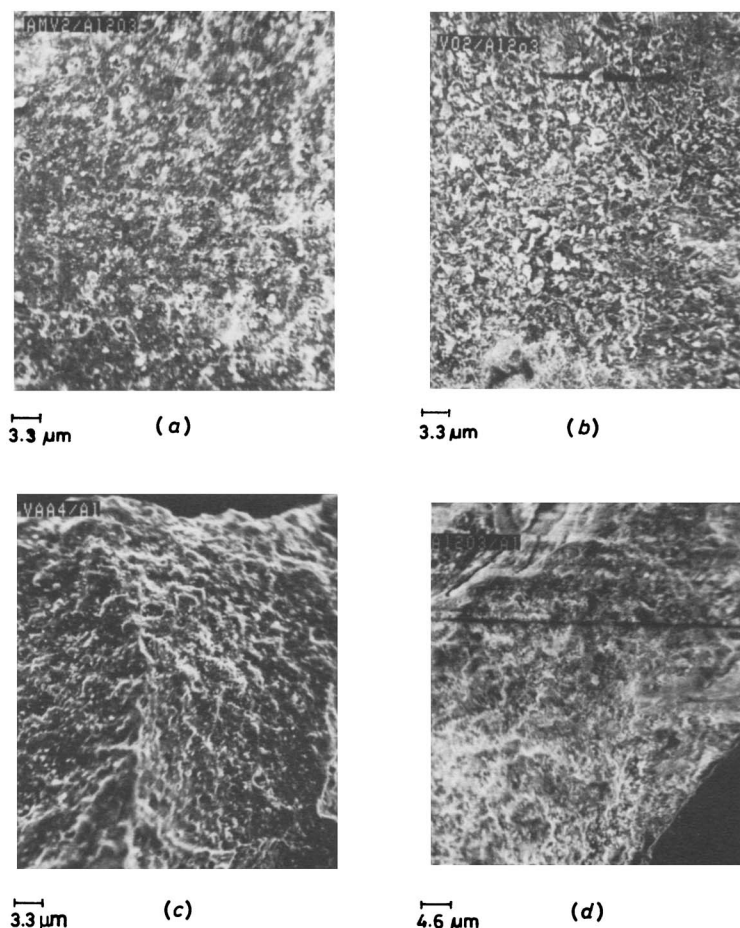
Fig. 4 Typical SEM micrographs of various samples: (a) AMV derived 2.22 wt.% $V_2O_5/\alpha-Al_2O_3$ (70 000 ×), (b) VOX derived 2.23 wt.% $V_2O_5/\alpha-Al_2O_3$ (70 000 ×), (c) VAA derived 2.21 wt.% $V_2O_5/\alpha-Al_2O_3$ (70 000 ×), (d) $\alpha-Al_2O_3$ (50 000 ×)

was greater, probably due to effective carrier–catalyst interaction when VAA was used for impregnating the $\alpha-Al_2O_3$ support. The hyperfine splitting values of both $A_\parallel$ and $A_\perp$ of this broad resonance were comparable with $\gamma-Al_2O_3$ supported V_2O_5 catalysts.[21] This broad resonance can be assumed to result from greater delocalization of the unpaired electron on the $\alpha-Al_2O_3$ support and suggests formulation of the paramagnetic centre as $(V \cdots O)^{2+}$ rather than V^{4+}. These centres formulated from EPR studies are deemed to be reacting with the 3-picoline molecules adsorbed on the surface of catalysts during ammoxidation. The dispersion and relative proportion of these paramagnetic centres are greater in the VAA-derived series of catalysts because the experimental rates of 3-picoline conversion are higher for this series of catalysts.

Oxygen Chemisorption and Ammoxidation Activity

The low-temperature oxygen chemisorption (LTOC) has been proved to be a facile technique for measuring dispersion of V_2O_5 on different supports.[14–16] In contrast to V_2O_5 supported on various other carriers,[14,15] for all three series of catalysts the oxygen uptake gradually increases with increase in V_2O_5 loading up to a certain level and then levels off with further loading (Fig. 6). There is seen to be a clear difference between the oxygen uptake capacities of the three series of catalysts. Even at low loadings of V_2O_5 the VAA-derived samples maintained a high oxygen-uptake trend. The best information to be obtained from the oxygen chemisorption

data was the active-site density (see Table 1, last column) which is found to be higher in the VAA-derived series than the other two series of catalysts. The active-site density, defined as the number of oxygen atoms chemisorbed per unit area of the reduced V_2O_5 surface, increases with increase in V_2O_5 loading and levels off at a certain loading irrespective of the source. The difference in active-site density between the three series of catalysts is also reflected in their catalytic activity for the rate of conversion of 3-picoline (Fig. 7). The rate of conversion of 3-picoline as a function of V_2O_5 loading is considerably more in the VAA derived series. This unusually high rate could be due to the formation of a highly dispersed active vanadia phase immobilization when VAA was taken as the impregnating agent for anchoring active vanadium oxide onto the surface of the $\alpha-Al_2O_3$ support. Similarly, the selectivity to nicotinonitrile remains high (Fig. 8) with this series of catalysts.

The rate of conversion of 3-picoline as well as the nicotinonitrile product selectivity increases, like the oxygen uptakes, with increase in vanadia loading up to a certain level then levels off. A direct correlation was also reported[29] earlier between oxygen-uptake capacities of various catalysts and the nicotinonitrile product selectivity. It has been established that oxygen, when chemisorbed at 195 K on the reduced vanadia catalysts, is dissociatively and selectively chemisorbed at the co-ordinatively unsaturated V oxide sites which are generated upon reduction in hydrogen.[14–15] According to the Mars and Van Krevelen[39] mechanism of sequential reduction and re-oxidation of the catalyst surface under steady-state conditions in oxidation reactions, the present
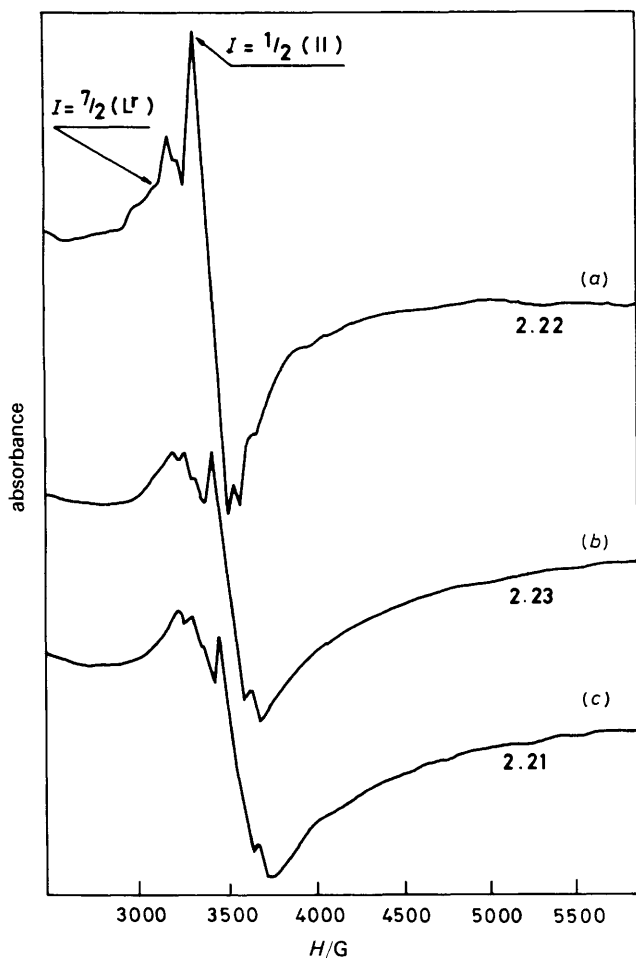
Fig. 5 EPR spectra of $V_2O_5/\alpha\text{-}Al_2O_3$ catalysts (a) AMV source, (b) VOX source, (c) VAA source

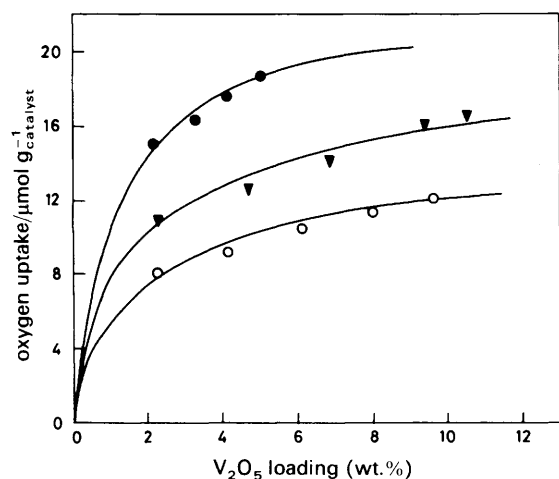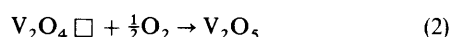ammoxidation sequence can be represented in terms of co-ordinatively unsaturated sites as in reactions (1) and (2).

$$3V_2O_5 + C_5H_4NCH_3 + NH_3$$

$$\rightarrow 3V_2O_4\square + C_5H_4NCN + 3H_2O \quad (1)$$

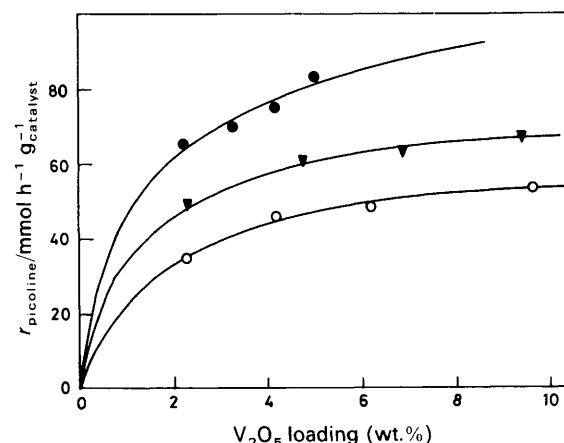$$V_2O_4\square + \tfrac{1}{2}O_2 \rightarrow V_2O_5 \quad (2)$$

Fig. 7 Rate of conversion of 3-picoline as a function of V_2O_5 loading: ●, VAA series; ▼, VOX series; ○, AMV series

Ammonia Chemisorption and Ammoxidation Activity

The choice of temperature at which ammonia adsorption could give useful information about the overall acidity of the catalysts was deemed crucial. Various authors have reported[40,41] different temperatures for measuring ammonia adsorption on V_2O_5-based catalysts. It was found necessary, however, in order to give reliable information about the overall acidity of these catalysts with chemisorbed ammonia, to choose a temperature as high as possible without oxidizing ammonia to any extent.[42,43] This limit of temperature seems meaningful because the 3-picoline ammoxidation was generally carried out between 623 and 673 K. The ammonia uptake on the three series of catalysts at 423 K gave three correlation lines with V_2O_5 loading on the support (Fig. 9). The $\alpha\text{-}Al_2O_3$ support contribution[44] to ammonia chemisorption was substracted before the results were reported. Impregnation of V_2O_5 onto the $\alpha\text{-}Al_2O_3$ carrier increased the ammonia-uptake capacities of the catalysts. Acidity of the catalysts is due mainly to the vanadia phase since ammonia uptake increases with increase in vanadia loading. The relation obtained can be explained in terms of stable Brønsted-acid centres which chemisorb ammonia as NH_4^+ and which are also of interest in the ammoxidation of 3-picoline.[20] It is clear from Fig. 9 that the number and nature of these centres are different for the three series of catalysts. The role of Brønsted-acid centres in the ammoxidation of 3-
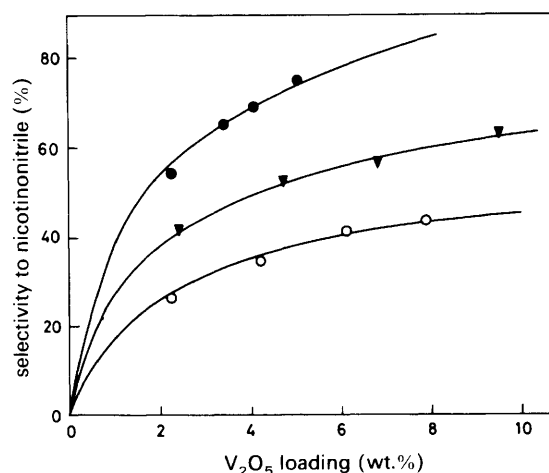

Fig. 6 Oxygen uptake at 195 K as a function of V_2O_5 loading: ●, VAA series; ▼, VOX series; ○, AMV series

Fig. 8 Selectivity to nicotinonitrile (%) plotted as a function of V_2O_5 loading of various catalysts: ●, VAA series; ▼, VOX series; ○, AMV series
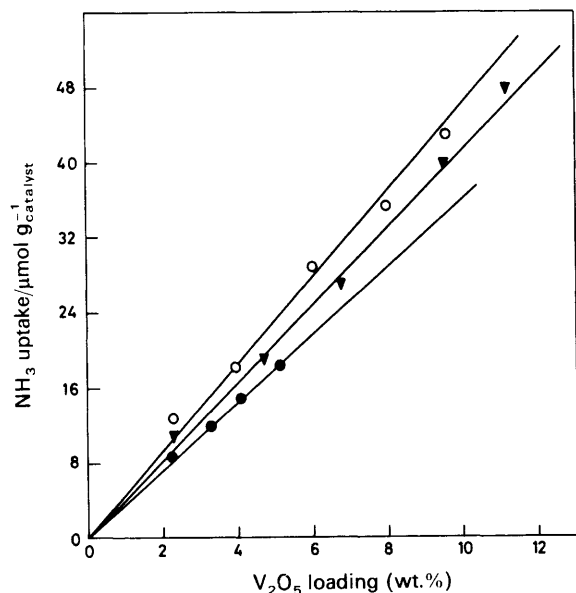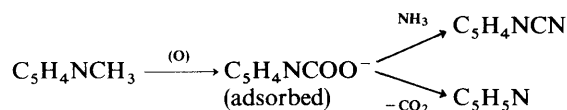
Fig. 9 Ammonia uptake as a function of V_2O_5 loading on the support of the three series of catalysts: ●, VAA series; ▼, VOX series; ○, AMV series

picoline can be better represented when we look at the selectivity to pyridine (a common byproduct in ammoxidation of picolines) on different catalysts as a function of ammonia uptake (Fig. 10). The pyridine formation can be shown with the help of the following scheme

$$C_5H_4NCH_3 \xrightarrow{(O)} \underset{\text{(adsorbed)}}{C_5H_4NCOO^-} \underset{-CO_2}{\overset{NH_3}{<}} \begin{array}{l} C_5H_4NCN \\ C_5H_5N \end{array}$$

The surface-adsorbed intermediate nicotinate ion, being more basic than ammonia, readily abstracts a proton from an adjacent Brønsted-acid site of V_2O_5 (the site is also responsible for ammonia chemisorption in the absence of this ion at lower temperatures) and thermally decarboxylates to pyridine. If the surface acidity is less, the nicotinate ion would find some time to react with gas-phase ammonia from the feed and produce a greater yield of nicotinonitrile. This mechanism appears to be operative in the case of all three
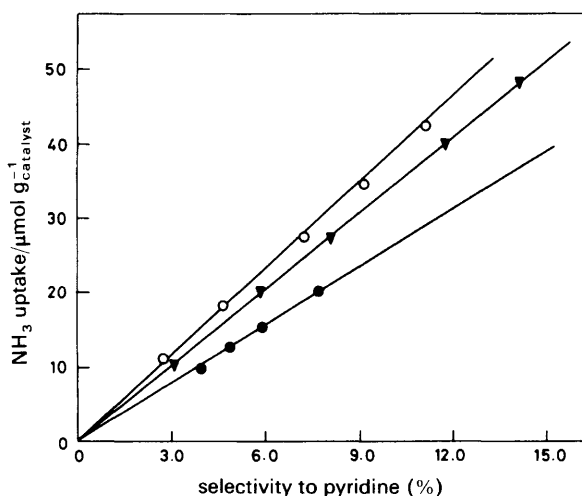
series of catalysts with the VAA-derived series producing more nicotinonitrile and less pyridine compared with the other two series of catalysts.

The variations in oxygen uptake and ammonia uptake with V_2O_5 loading obtained in this study for the three series of catalysts are in agreement with the literature. Combined, oxygen and ammonia uptakes give a reliable explanation of sites active during ammoxidation, and responsible for the selective formation of nicotinonitrile and pyridine, respectively, in the ammoxidation of 3-picoline.

Conclusions

In conclusion, we stress that vanadium(III) acetylacetonate can be used as a valuable precursor for impregnating low-surface-area supports like α-Al_2O_3 to give a more highly dispersed vanadia phase than that obtained with conventional vanadium sources, e.g. ammonium metavanadate and vanadyl oxalate. Oxygen chemisorption at low temperature can be used as a facile and readily accessible surface-specific probe for characterising the supported vanadia-based catalysts. In addition to oxygen chemisorption, other techniques, e.g. AES, SEM, EPR and XRD, could also be employed to give valuable information on the surface dispersion, structure and morphology of the vanadia-based ammoxidation catalysts. Finally, ammonia chemisorption can also be exploited to give information about the overall acidity and subsequent formation of pyridine (or benzene when the reactant is toluene) in various ammoxidation processes.

References

1 W. D. Mross, Ber. Bunsenges. Phys. Chem., 1984, **84**, 1042.
2 e.g. G. K. Boreskov in Proc. 1st Int. Sym. Scientific Bases for the Prepn. of Het. Catalysts, Brussels, October, 1975, ed. B. Delmon, P. Jacobs and G. Poncelet, Stud. Surf. Sci. Catal., 1976, **1**, 223.
3 V. V. Boldyrev, M. Buleng and B. Delmon, Stud. Surf. Sci. Catal., 1979, **2**, 7.
4 e.g. B. Delmon, Solid State Ionics, 1985, **16**, 243.
5 M. Che and L. Bonneviot in Successful Design of Catalysts, ed. T. Inui, Elsevier, Amsterdam, 1988, p. 147.
6 M. Komiyama, Catal. Rev. Sci. Eng., 1985, **27**, 341.
7 L. Forni, Appl. Catal., 1986, **20**, 219.
8 e.g. P. J. Gellings, in Catalysis, ed. G. C. Bond and G. Webb, Specialist Periodical Report, Royal Society of Chemistry, London, 1985, vol. 7, pp. 105.
9 I. E. Wachs, R. Y. Saleh, S. S. Chan and C. C. Chersich, Appl. Catal., 1985, **15**, 339.
10 D. Honicke, J. Catal., 1987, **105**, 10.
11 F. Cavani, F. Trifirò, P. Jiru, K. Habersberg and Z. Tvaruzkova, Zeolites, 1988, **8**, 12.
12 Bo Jonson, B. Rebenstorf, R. Larsson, S. L. T. Anderson and S. T. Lundin, J. Chem. Soc., Faraday Trans. 1, 1986, **82**, 767.
13 H. Miyata, K. Fujii, T. Ono, Y. Kubokawa, T. Ohno and F. Hatayama, J. Chem. Soc., Faraday Trans. 1, 1987, **83**, 675.
14 B. M. Reddy, K. Narsimha, P. Kanta Rao and V. M. Mastikhin, J. Catal., 1989, **118**, 22.
15 N. K. Nag, K. V. R. Chary, B. M. Reddy, B. R. Rao and V. S. Subrahmanyam, Appl. Catal., 1984, **9**, 225.
16 A. J. Vandillen, Ph.D. Thesis, University of Utrecht, 1977.
17 E. T. C. Vogt, M. Deboer, A. J. Vandillen and J. W. Geus, Appl. Catal., 1988, **40**, 255.
18 C. Martin and V. Rives, Adsorption Science and Technology, 1985, **2**, 241.
19 F. Roozeboom, M. C. Mittelmeijer-Hazeleger, J. A. Moulijn, J. Medema, V. H. J. de Beer and P. J. Gellings, J. Phys. Chem., 1980, **84**, 2783.

Fig. 10 Ammonia uptake vs. selectivity to pyridine (%) of the various catalysts: ●, VAA series; ▼, VOX series; ○, AMV series

20 A. Anderson, *J. Catal.*, 1982, **76**, 144.
21 K. V. R. Chary, B. M. Reddy, N. K. Nag, V. S. Subrahmanyam and C. S. Sunandana, *J. Phys. Chem.*, 1984, **88**, 2622.
22 M. Inomata, K. Mori, A. Miyamoto and Y. Murakani, *J. Phys. Chem.*, 1983, **87**, 754.
23 H. Miyata, M. Kohno, T. Ono, T. Ohno and F. Hatayama, *J. Chem. Soc., Faraday Trans. 1*, 1989, **85**, 3663.
24 M. Kotter, H. G. Lintz, T. Turek and D. L. Trimm, *Appl. Catal.*, 1989, **52**, 225.
25 R. A. Rajadhyaksha, G. Hausinger, H. Zeilinger, A. Ramstetter, H. Schmelz and H. Knözinger, *Appl. Catal.*, 1989, **51**, 67.
26 J. Kijenski. A. Baiker, M. Glinki, P. Dollenmeier and A. Wokaun, *J. Catal.*, 1986, **101**, 1.
27 J. Haber, A. Kozlowska and R. Kozkowski, *J. Catal.*, 1986, **102**, 52.
28 H. Van Hengstum, A. J. Van Ommen, J. G. Bosch and P. J. Gellings, *Appl. Catal.*, 1983, **5**, 207.
29 B. N. Reddy, B. M. Reddy and M. Subrahmanyam, *J. Chem. Soc., Chem. Commun.*, 1988, 33.
30 B. M. Reddy, K. V. R. Chary, V. S. Subrahmanyam and N. K. Nag, *J. Chem. Soc., Faraday Trans. 1*, 1985, **81**, 1655.
31 F. J. Szalkowski and G. A. Somorjai, *J. Phys. Chem.*, 1972, **56**, 6097.
32 C. N. R. Rao, D. D. Sharma and M. S. Hegde, *Proc. R. Soc. London, Ser. A*, 1980, **370**, 269.
33 C. N. R. Rao, *Philos. Trans. R. Soc. London, Ser. A*, 1986, **318**, 37.
34 J. A. Odriozola, H. Heinemann, G. A. Somorjai, J. F. Garcia de la Banda and P. Pereira, *J. Catal.*, 1989, **119**, 73.
35 M. M. Bhasin in *Catalyis in Organic Synthesis*, Academic Press, New York, 1976, p. 61.
36 D. M. Hercules and S. H. Hercules, *J. Chem. Educ.*, 1984, **61**, 487.
37 P. W. Palmberg, G. E. Riach, R. E. Weber and N. C. MacDonald in *Hand Book of Auger Electron Spectroscopy*, Physical Electronics Industries, Inc. Edina, Minn., 1972.
38 L. Forni, C. Oliva and C. Rebuscini, *J. Chem. Soc., Faraday Trans. 1*, 1988, **84**, 2398.
39 P. Mars and D. W. Van Krevelen, *Chem. Eng. Sci.*, Special Suppl., Proc. Conf. Oxid. Processes, 1954, **3**, 41.
40 B. M. Reddy and M. Subrahmanyam, *J. Chem. Soc., Chem. Commun.*, 1988, 940.
41 M. Ai, *J. Catal.*, 1978, **54**, 223.
42 N. I. Il'chenko and G. I. Golodets, *J. Catal.*, 1975, **39**, 57.
43 F. Theobald, R. Cabala and J. Bernard, *C.R. Seances Acad. Sci., Paris*, 1969, **269C**, 1209.
44 M. Niwa, H. Ando and Y. Murakami, *J. Catal.*, 1977, **49**, 72.